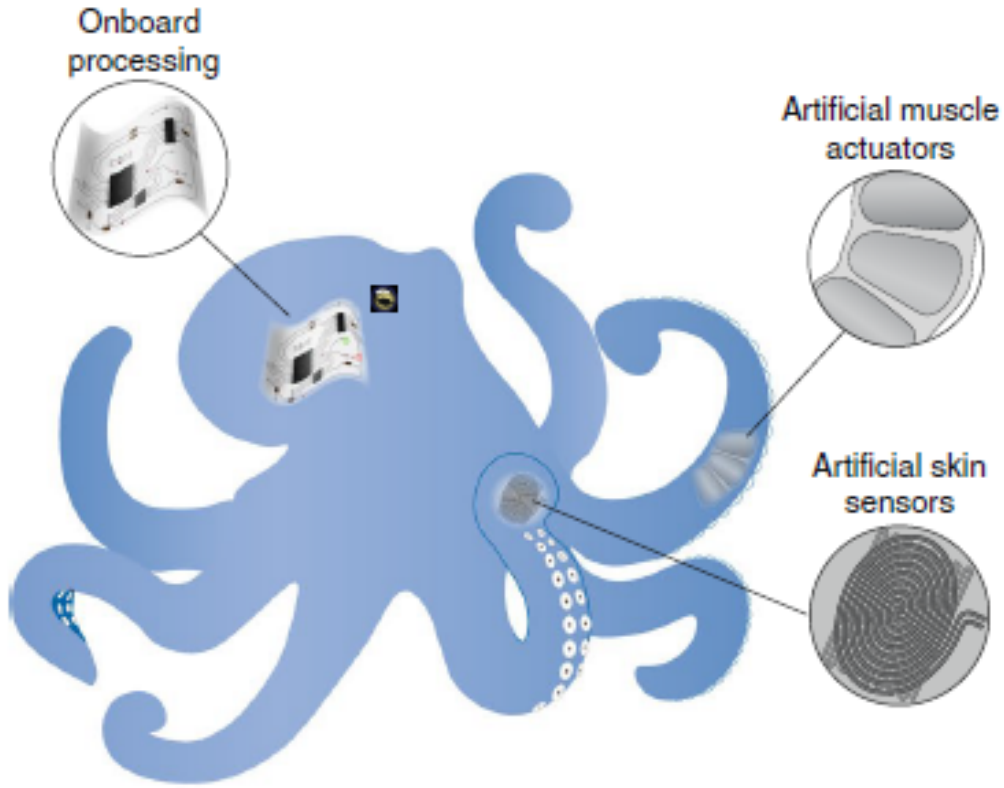


# Overview of Soft Robotics

Based on K.L.Johnson's book: Contact Mechanics

Ruzena Bajcsy

Spring 2020

**a****b**

Modality	Sensing and circuitry		Actuation	
	i	ii	iii	iv
Methods of achieving functionality				
	i	Unactuated	Actuated	Direction of actuation
Fluidic				
	$R = R_0$	$R > R_0$	$\Delta P = 0$ Inlet	$\Delta P > 0$ Air cavity (inflated)
Bio-hybrid				
	Chemosensitive bacteria	Chemical signals	$V = 0$	$V > 0$

**Fig. 1 | Overview of soft robotic systems.** **a**, Conception of a future soft robot, inspired by current state-of-the-art octopus-inspired robots<sup>5,6</sup>. This figure envisages the ways in which soft robotic technologies could be implemented in an advanced soft robot. **b**, Example methods of achieving circuitry and actuation for each generalized strategy (geometry-enabled, fluidic and bio-hybrid): (i) serpentine or wavy copper wiring between IC components that allow stretching; (ii) deterministic design of an auxetic metamaterial to create actuation in the  $y$ -direction in response to a force ( $F$ ) in the  $x$ -direction; (iii) microfluidic sensing enabled by the change in cross-sectional area of an EGaIn microchannel, which causes the resistance ( $R$ ) to increase from its initial value ( $R_0$ ); (iv) pneumatic actuation caused by the asymmetric expansion of air cavities under pressure, where  $\Delta P$  is the difference between pressure in the cavity and external pressure; (v) bio-hybrid sensing enabled by the luminescence of phytobacteria in response to chemical signals; and (vi) bio-hybrid actuation demonstrated when muscle cells contract under an applied voltage  $V$ .

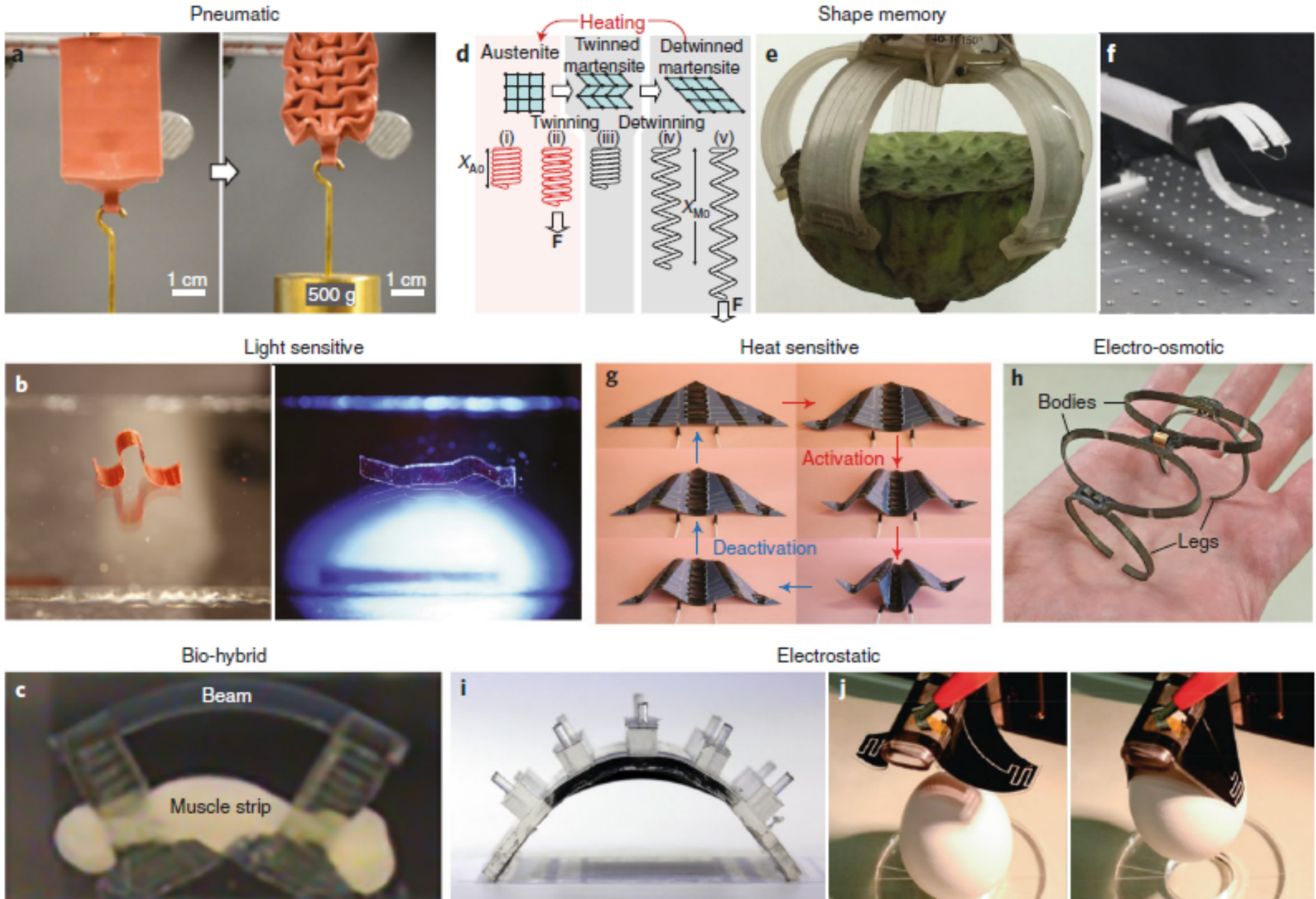
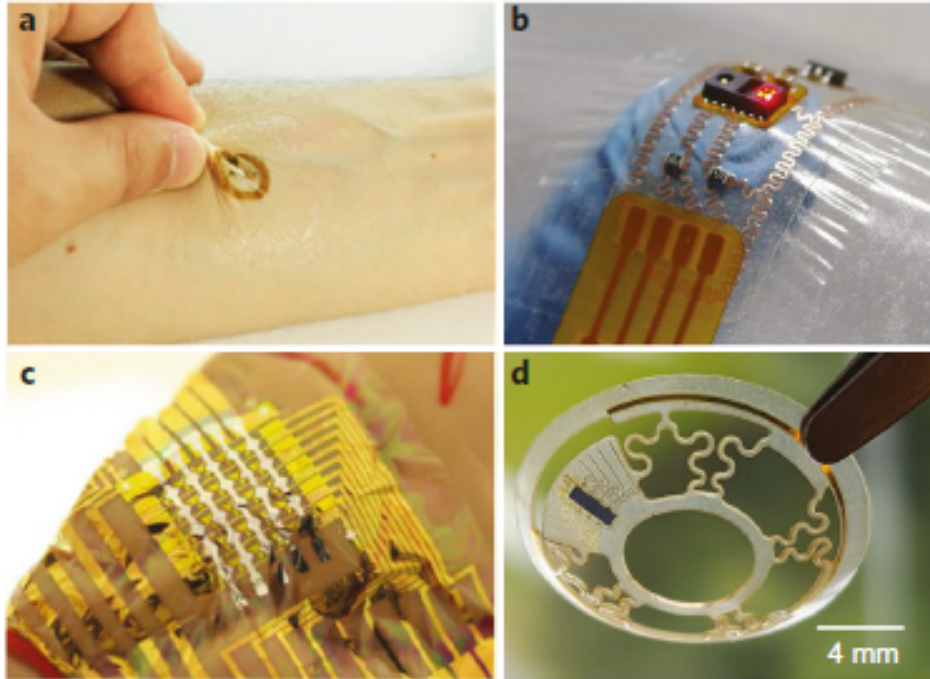
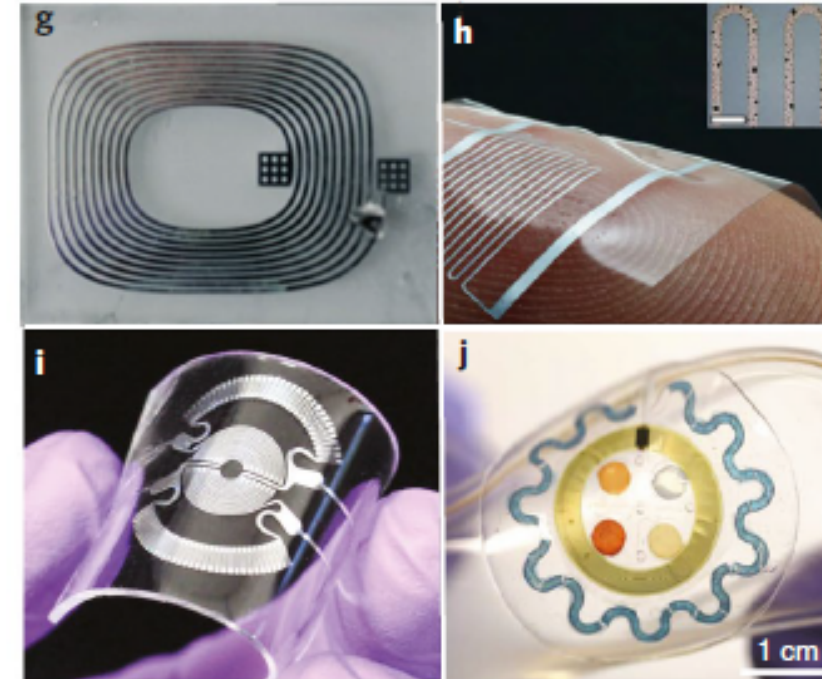


**Fig. 2 | Methods of soft actuation.** **a**, Vacuum-powered pneumatic actuator that creates contractile motion. **b**, A miniature LCE crawler (13 mm long) that moves in response to light. **c**, Bio-hybrid actuator (~4.6 mm long) with locomotion driven by electrically stimulated contraction of skeletal muscle. **d**, SMA spring, which contracts in response to resistive heating. In the diagram,  $F$  represents an applied force, while  $X_{A0}$  and  $X_{M0}$  represent the free length in the austenitic and martensitic spring, respectively. **e**, Modular gripper and walking robot actuated by resistive heating in an SMA. **f**, Gripper (100 mm long) actuated by resistive heating in a SMA. **g**, 3D-printed origami robot (110 mm side length) actuated by resistive heating in LCE hinges. **h**, Ionic polymer-metal composite-actuated caterpillar-inspired pipe crawling robot. **i**, Entirely soft, DEA-powered crawling robot (90 mm arc length). **j**, Dielectric elastomer actuator gripper, with increased gripping strength resulting from electrostatic adhesion. Credit: reproduced from ref. <sup>28</sup>, Wiley (**a**); ref. <sup>36</sup>, Wiley (**b**); ref. <sup>17</sup>, National Academy of Sciences (**c**); ref. <sup>51</sup>, IEEE (**d**); ref. <sup>52</sup>, IOP (**e**); ref. <sup>56</sup>, Elsevier (**f**); ref. <sup>59</sup>, Royal Society of Chemistry (**g**); ref. <sup>61</sup>, IEEE (**h**); ref. <sup>67</sup>, SPIE (**i**); ref. <sup>70</sup>, Wiley (**j**).

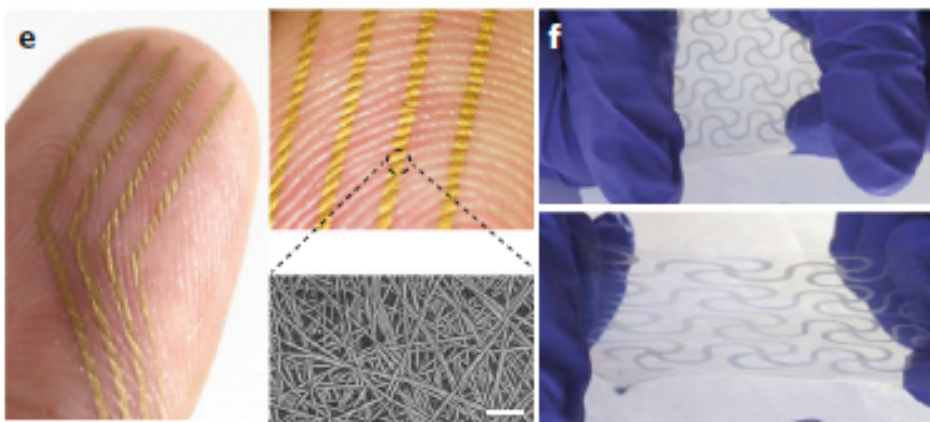
Ultrathin and deterministic materials



Soft microfluidic electronics



Nanomaterials



Ionic hydrogels

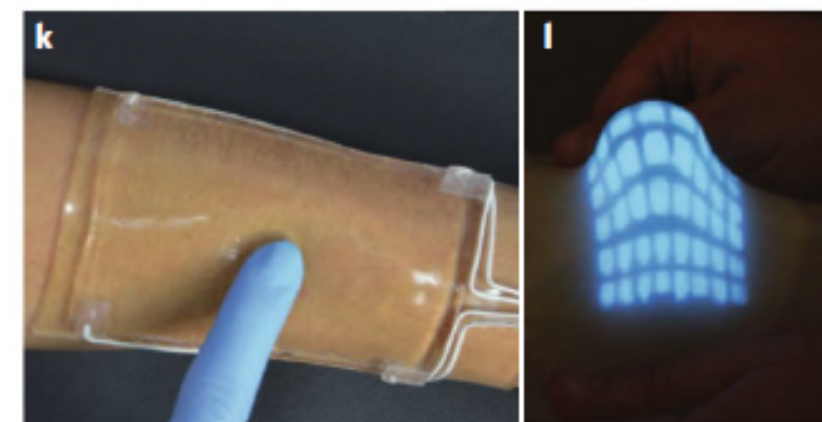


**Fig. 4 | Advances in soft sensing, conductivity and artificial skin.** **a-d**, Sensors fabricated from ultrathin and deterministic architectures. **e,f**, Conductive soft structures achieved by structured nanomaterials. Scale bar in **e**, 5  $\mu\text{m}$ . **g-j**, Conductive and wearable devices enabled by microfluidics. Scale bar in **h**, 5 mm. **k,l**, Wearable devices enabled by ionic hydrogel electronics. Specifically, these include: a mechano-acoustic on-skin sensor (**a**); a wearable device to measure electrophysiological signals and strain (**b**); an organic field-effect transistor/organic electrochemical transistor-enabled electrophysiology sensor array (**c**); a contact lens with integrated electronics (**d**); on-skin conductive traces that can measure strain and muscle activity (**e**); a highly stretchable PEDOT:PSS film applicable to transistor circuits (**f**); an EGaIn coil antenna fabricated by vacuum filling (**g**); a biphasic thin film of gold and gallium (**h**); a highly sensitive EGaIn-enabled pressure sensor (**i**); a colourimetric wearable patch for sweat analysis (**j**); a soft touch panel made from ionic hydrogels (**k**); and a stretchable LED array composed of 4 mm  $\times$  4 mm pixels, created from hydrogel and ZnS-doped dielectric elastomer (**l**). Credit: reproduced from ref. <sup>74</sup>, AAAS (**a**); ref. <sup>75</sup>, Wiley (**b**); ref. <sup>78</sup>, Wiley (**c**); ref. <sup>80</sup>, Wiley (**d**); ref. <sup>139</sup>, Macmillan Publishers Ltd (**e**); ref. <sup>97</sup>, AAAS (**f**); ref. <sup>104</sup>, Royal Society of Chemistry (**g**); ref. <sup>105</sup>, Wiley (**h**); ref. <sup>106</sup>, Wiley (**i**); ref. <sup>112</sup>, AAAS (**j**); ref. <sup>113</sup>, AAAS (**k**); ref. <sup>7</sup>, AAAS (**l**).

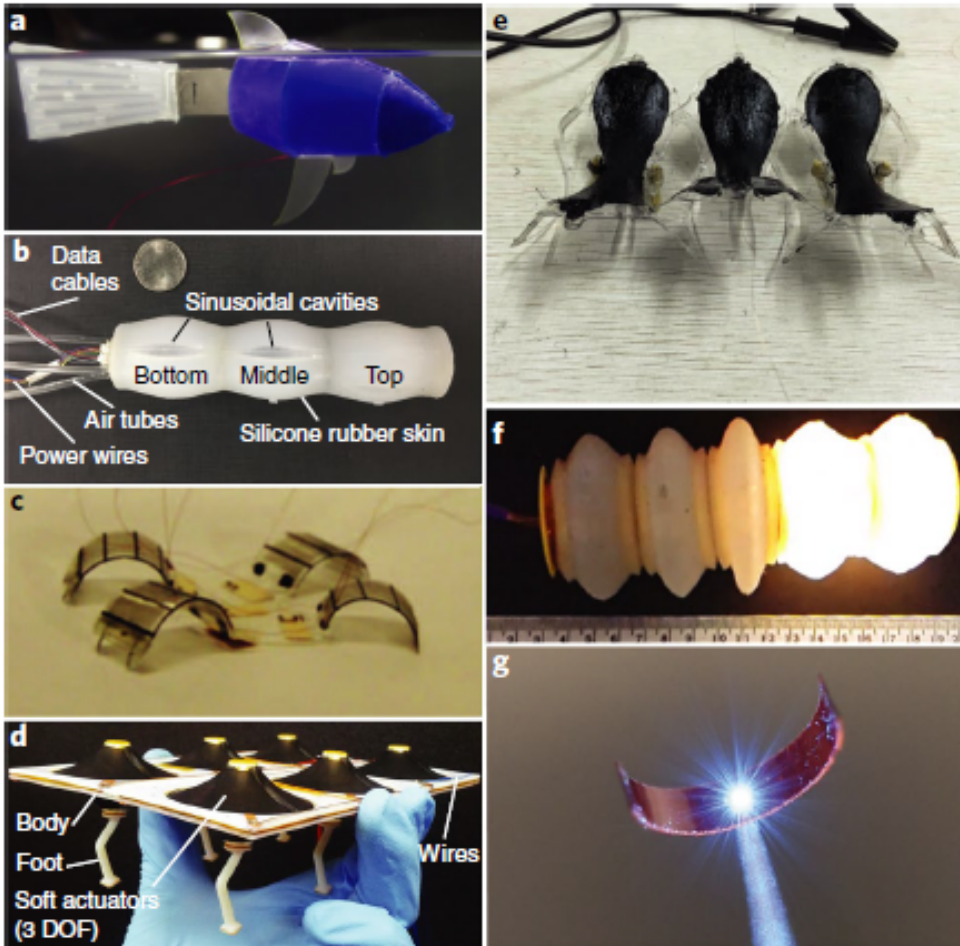


**Fig. 5 | Implementation of soft actuators into robotic systems.** **a**, SMA-actuated fish (20 cm long). **b**, SMA-actuated peristalsis robot (13.9 cm diameter). **c**, Fast DEA-actuated walker (6 cm). **d**, A multi-degree-of-freedom (DOF) DEA-powered walker. **e**, Differential friction, DEA-powered annelid robot (17 cm). **f**, Electromagnetically actuated pneumatic worm-robot. **g**, Venus flytrap-inspired, LCE-actuated gripper (5 mm). Credit: reproduced from ref.<sup>55</sup>, National Academy of Sciences (**a**); ref.<sup>54</sup>, IEEE (**b**); ref.<sup>63</sup>, IEEE (**c**); ref.<sup>68</sup>, Elsevier (**d**); ref.<sup>117</sup>, IOP (**e**); ref.<sup>32</sup>, Mary Ann Liebert (**f**); ref.<sup>35</sup>, Macmillan Publishers Ltd (**g**).

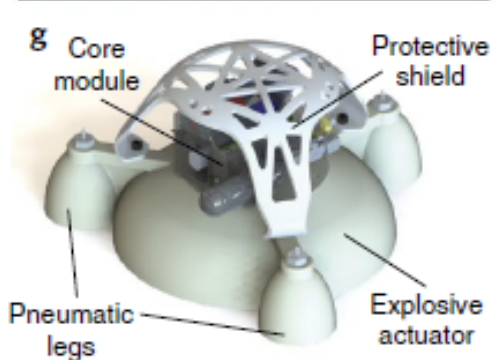
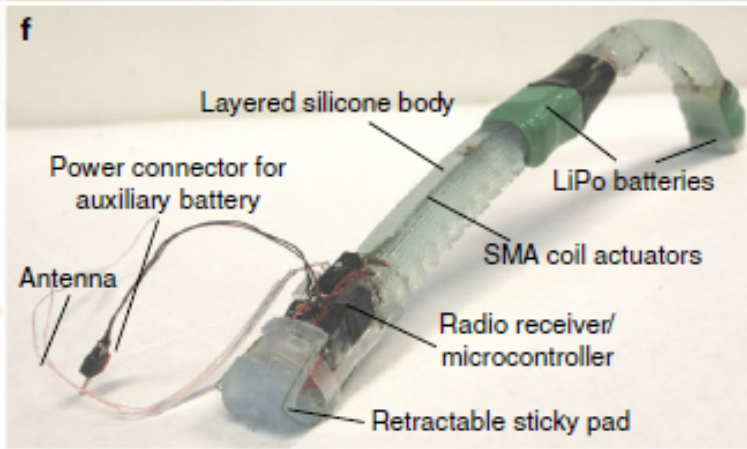
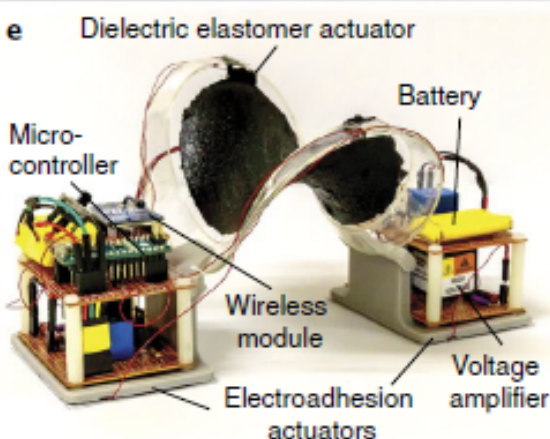
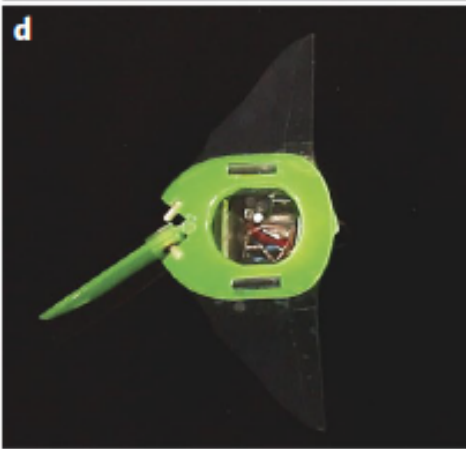
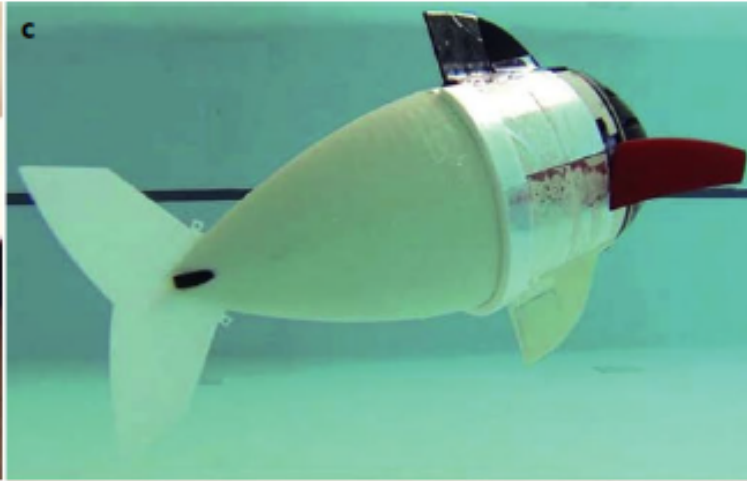
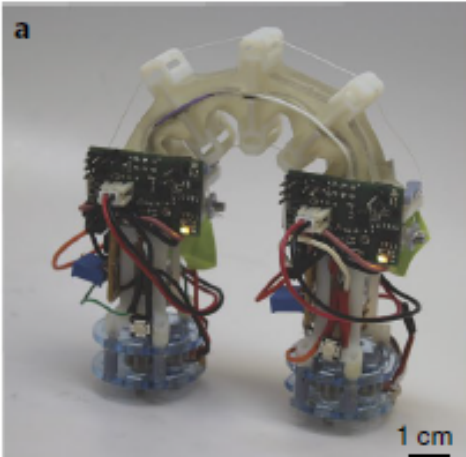
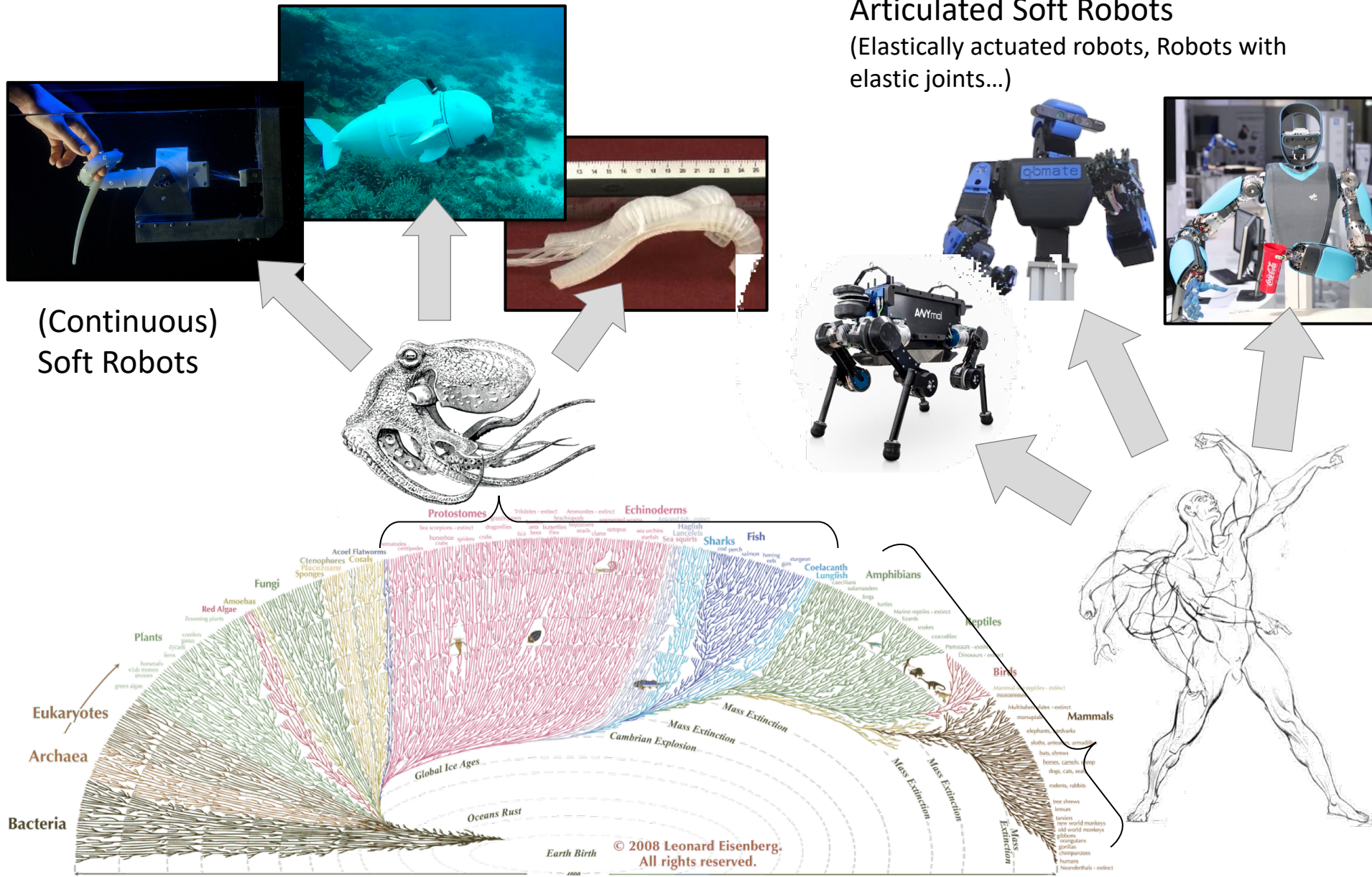


**Fig. 6 | Fully untethered robotic systems.** **a**, Climbing robot powered by a motor-cable system. **b**, Robust walking robot powered by on-board pneumatics (65 cm long). **c**, Biomimetic swimming robot powered by a hydraulic actuation system (35 cm long). **d**, Ray-inspired swimming robot powered by DEAs (9.3 cm long). **e**, Electro-adhesive walking robot powered by DEAs. (17 cm outer diameter) **f**, Caterpillar-inspired multi-gait robot powered by SMAs (10 cm long). **g**, Jumping robot powered by combustion (12.6 cm tall; 30 cm radius). **h**, Jumping robot with controllable orientation powered by combustion (8 cm tall; 15 cm radius). **i**, Octopus robot powered by combustion and controlled by fluidic logic (~55 mm). Credit: reproduced from ref.<sup>118</sup>, IEEE (**a**); ref.<sup>22</sup>, Mary Ann Liebert (**b**); ref.<sup>119</sup>, Mary Ann Liebert (**c**); ref.<sup>65</sup>, AAAS (**d**); ref.<sup>123</sup>, SPIE (**e**); ref.<sup>122</sup>, IOP (**f**); ref.<sup>42</sup>, AAAS (**g**); ref.<sup>31</sup>, IEEE (**h**); ref.<sup>12</sup>, Macmillan Publishers Ltd (**i**).

# Elastic bodies inspired by nature



# Dynamic and precise motions



Rigid Robots > Soft Robots

# Dynamic and precise motions



Rigid Robots > Soft Robots



$$B(q)\ddot{q} + C(q, \dot{q})\dot{q} + G(q) = \tau \quad \text{Very well understood dynamic behavior!}$$

# Compliance through Elastic Materials

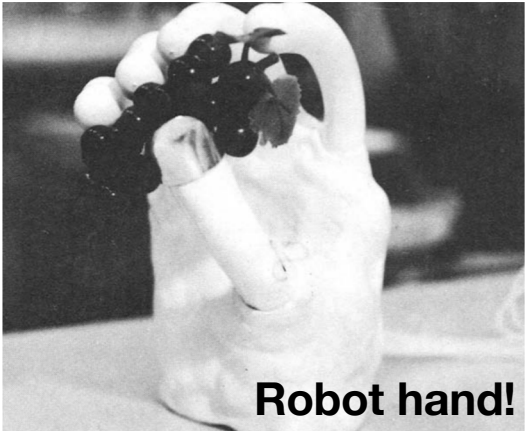
---

Elastic materials producing compliant robots

Koichi Suzumori

*Toshiba Corporation, 4-1 Ushimado-cho, Kawasaki-ku, Kawasaki 210, Japan*

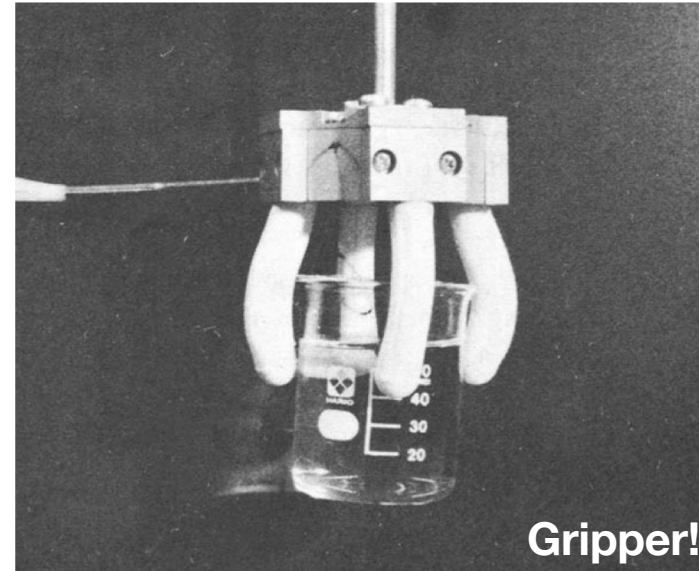
(1996)



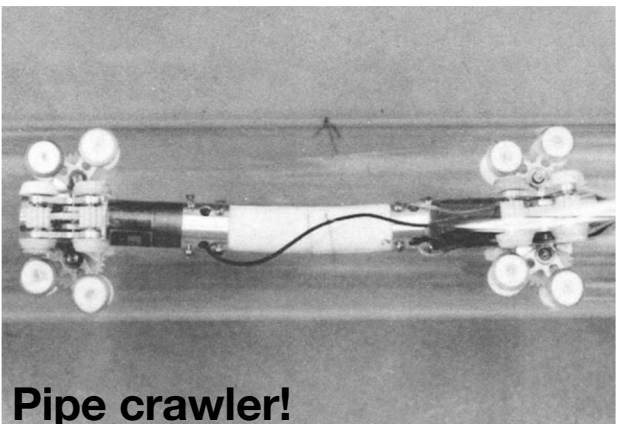
**Robot hand!**



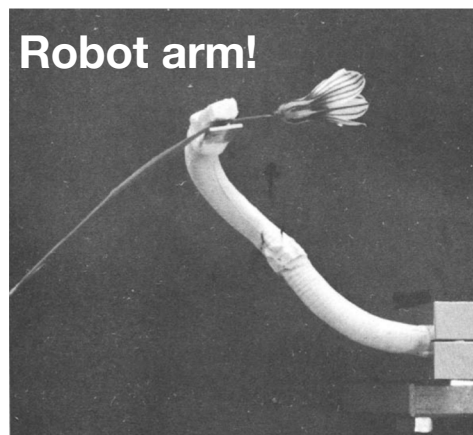
**Small walker!**



**Gripper!**



**Pipe crawler!**



**Robot arm!**



**Big walker!**

# Introduction

- While *Classical Mechanics* deals solely with bulk material properties *Contact Mechanics* deals with bulk properties that consider surface and geometrical constraints.
- It is in the nature of many rheological tools to probe the materials from "outside". For instance, a probe in the form of a pin in a pin-on-disk tester is brought into contact with the material of interest, measuring properties such as hardness, wear rates, etc.
- Geometrical effects on local elastic deformation properties have been considered as early as 1880 with the *Hertzian Theory of Elastic Deformation*.<sup>1</sup> This theory relates the circular contact area of a sphere with a plane (or more general between two spheres) to the elastic deformation properties of the materials. In the theory any surface interactions such as near contact *Van der Waals* interactions, or contact *Adhesive* interactions are neglected.

# Contact Mechanics from Wikipedia

- **Contact mechanics** is the study of the [deformation of solids](#) that touch each other at one or more points.[\[1\]](#)[\[2\]](#) A central distinction in contact mechanics is between [stresses](#) acting [perpendicular](#) to the contacting bodies' surfaces (known as the [normal direction](#)) and [frictional](#) stresses acting [tangentially](#) between the surfaces. This page focuses mainly on the normal direction, i.e. on frictionless contact mechanics. [Frictional contact mechanics](#) is discussed separately. Normal stresses are caused by applied forces and by the [adhesion](#) present on surfaces in close contact even if they are clean and dry.

# Hertzian Contact

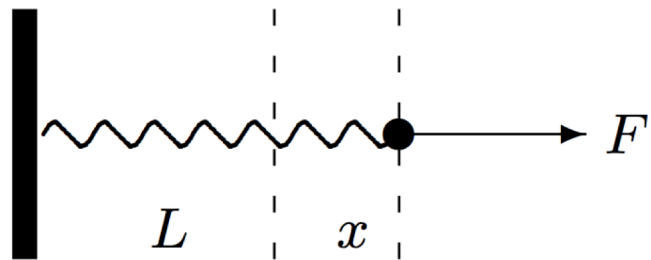
- Hertzian contact stress refers to the localized stresses that develop as two curved surfaces come in contact and deform slightly under the imposed loads. This amount of deformation is dependent on the modulus of elasticity of the material in contact. It gives the contact stress as a function of the normal contact force, the radii of curvature of both bodies and the modulus of elasticity of both bodies. Hertzian contact stress forms the foundation for the equations for load bearing capabilities and fatigue life in bearings, gears, and any other bodies where two surfaces are in contact.

# Linear Elasticity

**Strain:** normalized extension ( $dx/x_0$ )

**Stress:** the cause of strain (force on a surface)

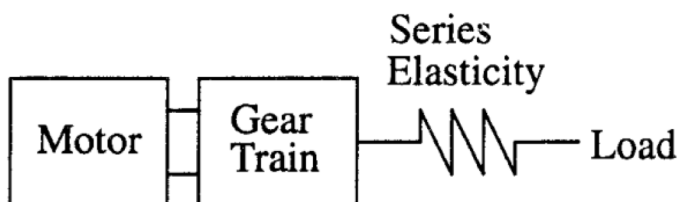
## Elastic Mechanical Linkage



$$F = kx$$

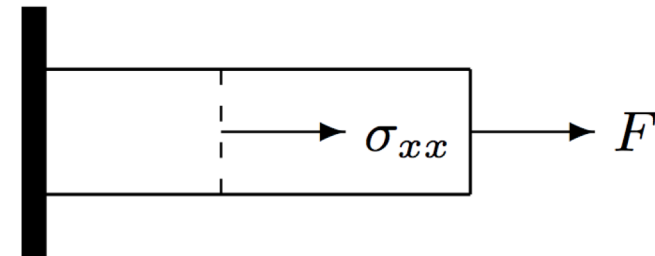
(stress = (constitutive relation) \* strain)

## Series Elastic Actuator (Pratt)



## Soft Material

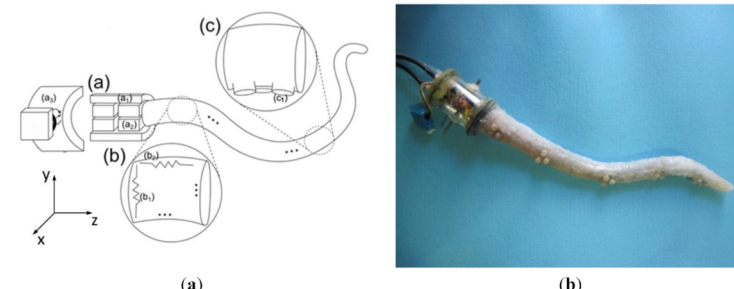
(Infinitely many springs with infinitesimal rest length)



$$\sigma_{ij} = \sum_{kl} E_{ijkl} u_{kl}$$

(convenient way to lots of spring equations)

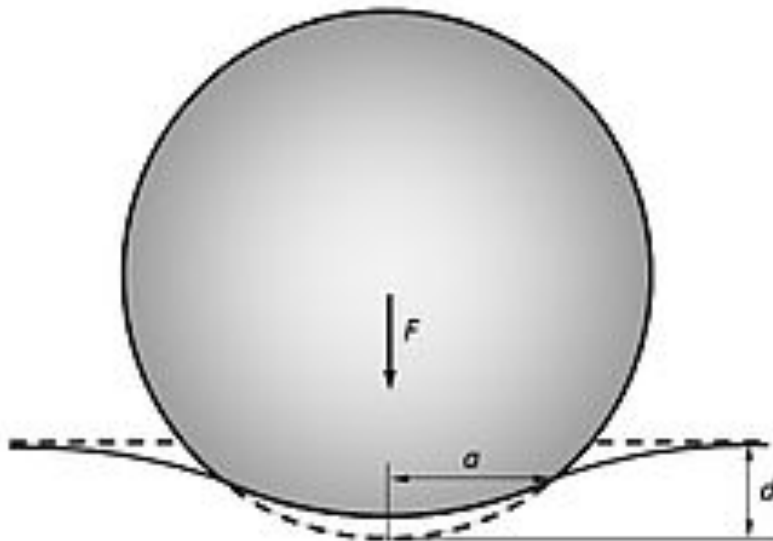
## Soft Robot Arm (Laschi)



Contact between a sphere and a half-space

Contact of an elastic sphere with an elastic half-space

An elastic sphere of radius  $R$  indents an elastic half-space to depth  $d$ , and thus creates a contact area of radius



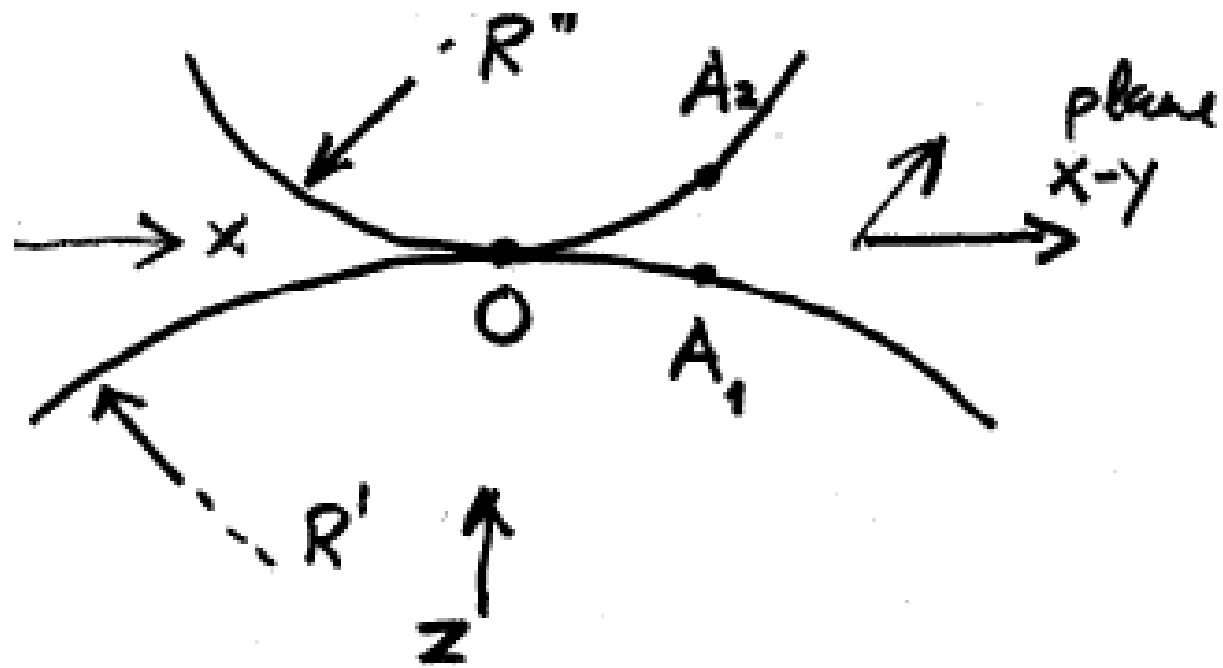
# Hertz's Elastic Theory of Contact

Consider two bodies with radii of curvature  $R'$  and  $R''$ .

- 1) Before deformation the bodies touch at O, and the separation of points  $A_1$  and  $A_2$  is

$$h = |A_2 - A_1| = \frac{1}{2R'} x^2 + \frac{1}{2R''} y^2$$

Two bodies in contact A<sub>1</sub>,A<sub>2</sub> at point O

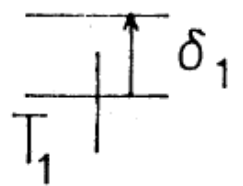
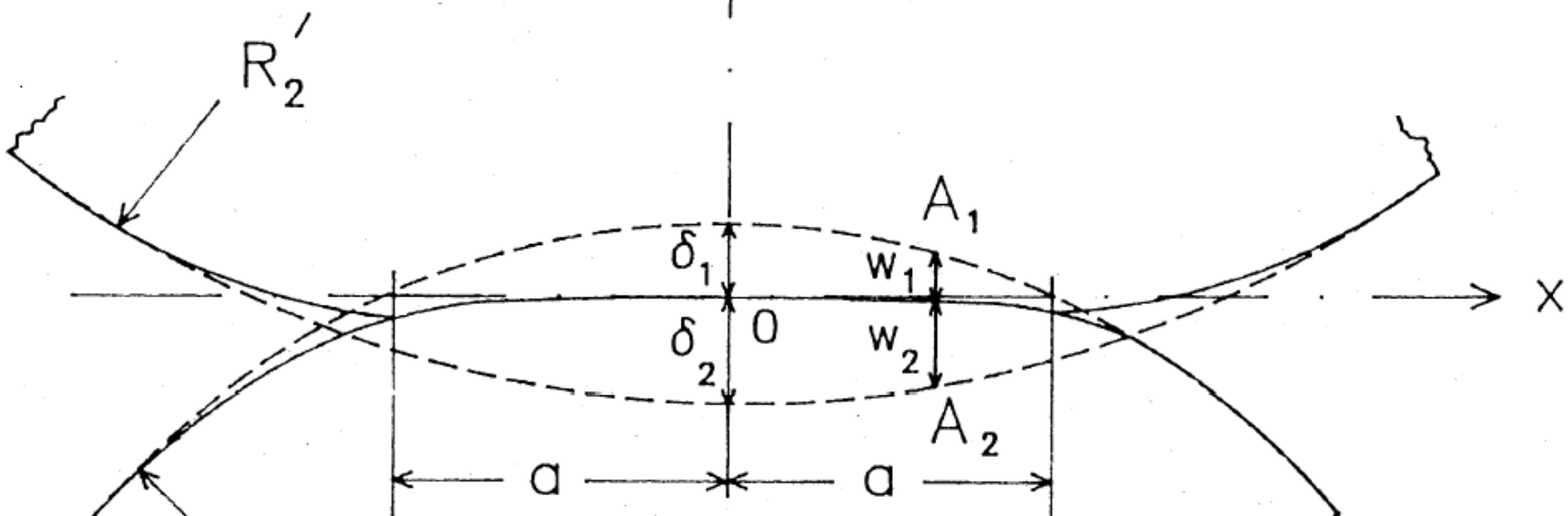
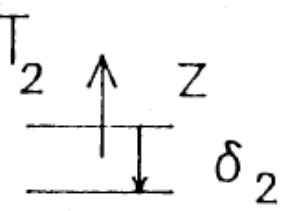


Next slide has the complete picture from Johnson's book

- 2) Applying a normal load, the two bodies are compressed. The separation at  $A_1$  and  $A_2$  is now

$$h' = h - (S_1 + S_2) + (w_1 + w_2)$$

$w_1$  and  $w_2$  are the normal elastic displacements of the surface at  $A_1$  and  $A_2$   
 $S_1$  and  $S_2$  correspond to the displacement of the distant points of each body



# Assumptions of Hertz's theory

- 1. He assumed Elastic Half-space loaded over a region(circular/elliptical) generally followed by Contact Stress theory.
- Two conditions must be satisfied:
- A) contact area must be small relative with the dimension of each body
- B) The relative radii of the curvature must be small. This implies the stress field calculation on the basis of solid which is infinite in extent is not seriously influenced by the proximity of its boundaries to the highly stressed region. Metallic solids comply to this condition but rubber NOT.

# Theory cont.

- Finally, it is assumed that surfaces are frictionless which implies the normal pressure is transmitted fully between the two bodies.
- The Linear theory of elasticity does not account for changes in the boundary forces arising from deformation. The Normal traction at the interface are taken to act parallel to the axis, tangential acts in x-y plane.
- Contact area is a. the relative radius is  $R$ , significant radii of each body are  $R[1], R[2]$  and depth is  $l$ .

# Theory, cont.

- The assumptions of Hertz theory are; The surfaces are continuous and non-conforming  $a \ll R$
- The strains are small : $a \ll R$
- Each solid can be considered as an elastic half space:  $a \ll R$ ,  $a \ll l$
- The surfaces are frictionless : $q[x]=q[y]=0$
- The problem of elasticity can be stated: The distribution of mutual pressure  $p(x,y)$  acting over an area  $S$  on the surface of two elastic half surfaces is required which will produce normal displacement of the surfaces  $u[z_1]$  and  $u[z_2]$  satisfying equation (4.7) with  $S$  and (4.8) outside.

## Hertz .2

(i) If points  $A_1$  and  $A_2$  are within the contact area  $\Rightarrow h' = 0$

$$\Rightarrow \boxed{w_1 + w_2 = (\delta_1 + \delta_2) - h}$$

elastic displacement of bodies separation of  $A_1$  and  $A_2$  for single point contact

$$\Rightarrow \boxed{w_1 + w_2 = \delta - \frac{x^2}{2R'} - \frac{y^2}{2R''}}$$

$$\delta \equiv \delta_1 + \delta_2 = w_1(0) + w_2(0)$$

(corresponds to the approach of two distant points)

(ii) If  $A_1$  and  $A_2$  are outside the contact area  
 $\Rightarrow h' > 0$

$$\Rightarrow \boxed{w_1 + w_2 > \delta - \frac{x^2}{2R'} - \frac{x^2}{2R''}}$$

3) The resultant force transmitted from one surface to the other through the contact areas is resolved into

- a normal load  $L$
- tangential force components  $Q_x$  and  $Q_y$  sustained by friction

It is:  $L = \int_S p dS$ ;  $p$  normal traction (pressure)

$$Q_x = \int_S q_x dS; \quad q_x, q_x \text{ lateral traction}$$

$$Q_y = \int_S q_y dS;$$

### A. Contact between a sphere and an elastic half-space

As showed in Figure 1, an elastic sphere of radius  $R$  indents an elastic half-space to depth  $u$ , and thus creates a contact area of radius  $a \cong (\frac{3RF}{2E_*})^{1/3}$ .

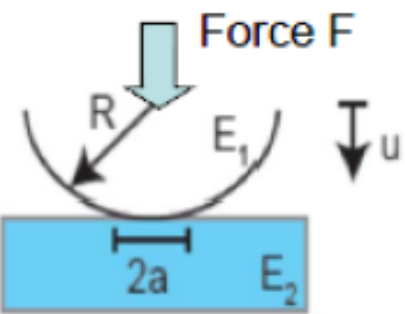


Fig. 1. Contact stress

The depth of indentation  $u$  is given by:  $u \cong (\frac{2F^2}{E_*^2 R})^{1/3}$

where

$$\frac{1}{E_*} = \frac{1}{2} \left( \frac{1 - v_1^2}{E_1} + \frac{1 - v_2^2}{E_2} \right)$$

And  $E_1, E_2$  are the elastic moduli and  $v_1, v_2$  the Poisson's ratios associated with each body.

Stiffness:  $k = \frac{dF}{du} \cong (E_*^2 RF)^{1/3}$

Stress:  $(\sigma_c)_{max} \cong \frac{3}{2} \frac{F}{\pi a^2} = 0.4 \left( \frac{E_*^2 F}{R^2} \right)^{\frac{1}{3}} = 0.4 \frac{k}{R}$

$$\tau_{max} \cong \frac{(\sigma_c)_{max}}{3}$$

### C. Contact between two cylinders with parallel axes

Figure 3 showed the contact between two cylinders with the radii of  $R_1$  and  $R_2$  with parallel axes.

In contact between two cylinders, the force is linearly proportional to the indentation depth.

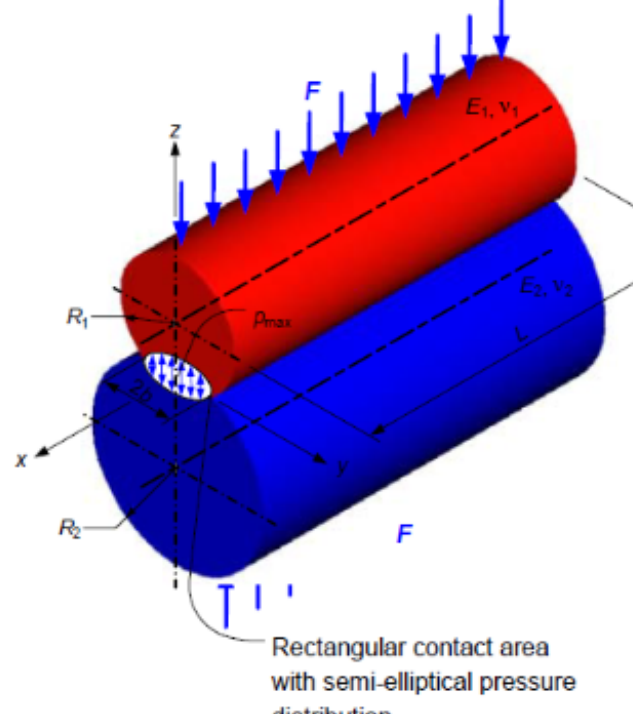


Fig. 3. Contact between two cylinders

The half-width  $b$  of the rectangular contact area of two parallel cylinders is found as:

$$b = \sqrt{\frac{4F\left[\frac{1-v_1^2}{E_1} + \frac{1-v_2^2}{E_2}\right]}{\pi L\left(\frac{1}{R_1} + \frac{1}{R_2}\right)}}$$

Where  $E_1$  and  $E_2$  are the moduli of elasticity for cylinders 1 and 2 and  $v_1$  and  $v_2$  are the Poisson's ratios, respectively.  $L$  is the length of contact.

The maximum contact pressure along the center line of the rectangular contact area is:

$$P_{max} = \frac{2F}{\pi bL}$$

The equilibrium load  $L = \int p(r) dS = \int p_0 \sqrt{1-r^2/a^2} dS$



$$L = \int_0^a p_0 \sqrt{1-r^2/a^2} 2\pi r dr = \frac{2}{3} p_0 \pi a^2$$

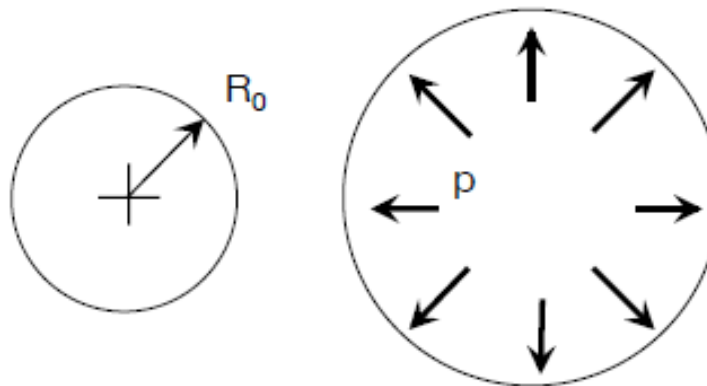
$\Rightarrow$  Hertz Equations for Elastic Contact:

radius of contact  $a = \left[ \frac{3LR}{4E^*} \right]^{1/3}$

mutual approach  
of distant points  $S = \frac{a^2}{R} = \left[ \frac{9L^2}{16RE^{*2}} \right]^{1/3}$

max. pressure  
 $P_m$  mean pressure  $p_0 = \frac{3L}{2\pi a^2} = \frac{3}{2} P_m = \left[ \frac{6LE^{*2}}{\pi^3 R^2} \right]^{1/3}$

## Sphere Inflation



Equibiaxial Loading:

$$\lambda_1 = \lambda_2 = \lambda \equiv \frac{R}{R_0} \quad \lambda_3 = \frac{1}{\lambda_1 \lambda_2} = \frac{1}{\lambda^2}$$

$$W = W(\lambda_1, \lambda_2, \lambda_3)$$

$$\Pi = \Pi(R) = 4\pi R_0^2 t_0 W - \frac{4}{3}\pi R^3 p$$

$$\frac{d\Pi}{dR} = 0 \Rightarrow p = \frac{t_0 R_0^2}{R^2} \frac{dW}{dR}$$

## Constitutive Laws

NeoHookean

$$W = \frac{E}{6} (\lambda_1^2 + \lambda_2^2 + \lambda_3^2 - 3)$$

“1-param” Ogden

$$W = \frac{E}{24} (\lambda_1^4 + \lambda_2^4 + \lambda_3^4 - 3)$$

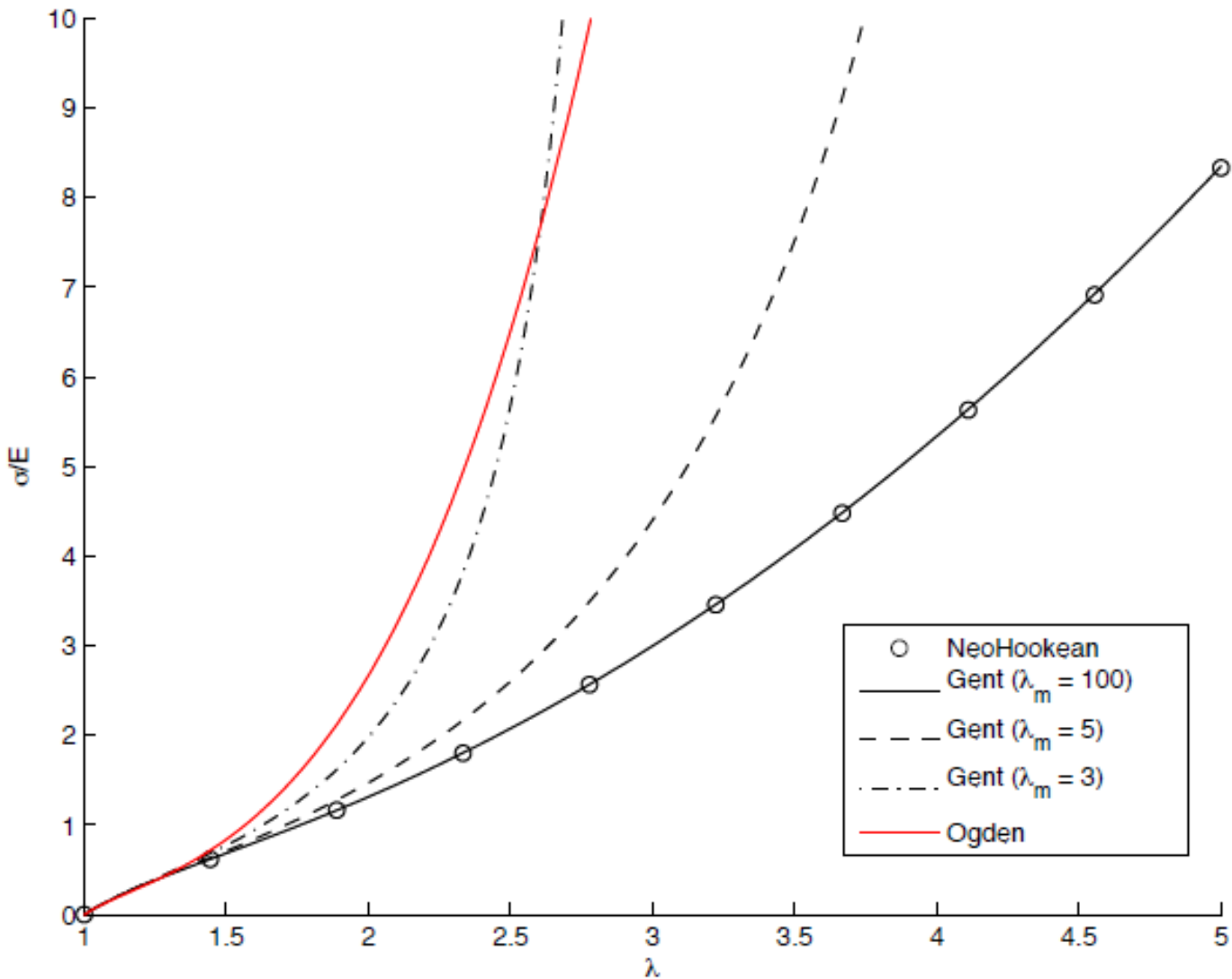
“Gent” Solid

$$W = -\frac{EJ_m}{6} \ln\left(1 - \frac{J_1}{J_m}\right)$$

$$J_1 = \lambda_1^2 + \lambda_2^2 + \lambda_3^2 - 3$$

$J_m$  = maximum possible value of  $J_1$   
due to strain hardening

# Stress-Stretch



# References

- Steven I. Rich, Robert J. Wood and Carmel Majidi:
- Untethered Soft Robotics , Review article ,  
<https://doi.org/10.1038/s41928-018-0024-1>